NANO LETTERS

Letter

pubs.acs.org/NanoLett

Conjugated Block Copolymer Photovoltaics with near 3% Efficiency through Microphase Separation

Changhe Guo,[†,¶] Yen-Hao Lin,[§,¶] Matthew D. Witman,[†] Kendall A. Smith,[§] Cheng Wang,[∥] Alexander Hexemer,[∥] Joseph Strzalka,[⊥] Enrique D. Gomez,*[,†,‡] and Rafael Verduzco*[,§]

[†]Department of Chemical Engineering and [‡]Materials Research Institute, The Pennsylvania State University, University Park, Pennsylvania 16802, United States

[§]Department of Chemical and Biomolecular Engineering, Rice University, Houston, Texas 77005, United States

[∥]Advanced Light Source, Lawrence Berkeley National Laboratory, Berkeley, California 94720, United States

[⊥]X-ray Science Division, Argonne National Laboratory, Argonne, Illinois 60439, United States

S *Supporting Information*

ABSTRACT: Organic electronic materials have the potential to impact almost every aspect of modern life including how we access information, light our homes, and power personal electronics. Nevertheless, weak intermolecular interactions and disorder at junctions of different organic materials limit the performance and stability of organic interfaces and hence the applicability of organic semiconductors to electronic devices. Here, we demonstrate control of donor−acceptor heterojunctions through microphase-separated conjugated block copolymers. When utilized as the active layer of photovoltaic cells, block copolymer-based devices demonstrate efficient photoconversion well beyond devices composed of homopolymer blends. The 3% block copolymer device efficiencies are achieved without the use of a fullerene acceptor. X-ray scattering results reveal that the remarkable performance of block copolymer solar cells is due to self-assembly into mesoscale lamellar morphologies with primarily face-on crystallite orientations. Conjugated block copolymers thus provide a pathway to enhance performance in excitonic solar cells through control of donor−acceptor interfaces.

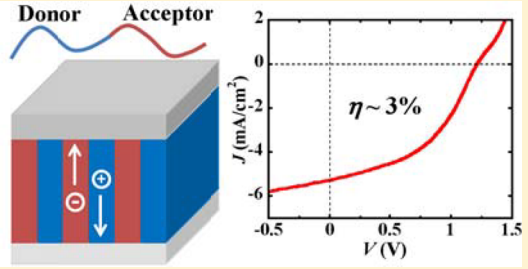

KEYWORDS: *Self-assembly, organic solar cells, all-conjugated block copolymers, RSOXS, GIWAXS*

Excitonic photovoltaics are a class of devices where donor−acceptor interfaces are critical for photogeneration of charges and efficient device performance.[1−4] In contrast to many inorganic semiconductors where optical excitations generate delocalized free charge carriers, current generation in organic photovoltaics depends on dissociation of tightly bound charge transfer states near donor−acceptor interfaces. For instance, a recent model by Giebink et al. suggests that tuning the electronic coupling at donor/acceptor interfaces is crucial to minimizing the recombination rate of charge transfer states while maintaining yields of exciton dissociation near unity.[5] It follows that tuning the chemical structure and local order at organic heterojunctions is a requirement to access the full potential of organic solar cell materials. Unfortunately, organic solar cells rely on kinetically trapped, partially phase-separated structures of donor/acceptor mixtures to create a high surface area for exciton dissociation and networks of bicontinuous phases for charge extraction.[6−12] As a consequence, molecular control of the interface in state-of-the-art organic photovoltaics is nearly impossible.

Microphase-separated block copolymers comprised of electron donor and electron acceptor polymers can address many of the current challenges in morphology and interfacial structure control for photovoltaics. The equilibrium self-assembly of block copolymers into mesoscale (5−500 nm) well-ordered morphologies where interfaces are governed by moieties near the junction between blocks[13,14] is ideal for the active layer of organic solar cells. While several examples of block copolymers with donor and acceptor blocks have been reported, the majority contain a nonconjugated insulating backbone in at least one polymer block and consequently do not directly control donor/acceptor interfaces.[15−20] Recent work has demonstrated significant progress in the design, synthesis, and characterization of fully conjugated block copolymers,[21−23] but it remains a challenge to achieve efficient charge photogeneration in photovoltaic device architectures.

We demonstrate that poly(3-hexylthiophene)−*block*−poly((9,9-dioctylfluorene)-2,7-diyl-alt-[4,7-bis(thiophen-5-yl)-2,1,3-benzothiadiazole]-2′,2″-diyl) (P3HT-*b*-PFTBT) block copolymers can be utilized as the active layer for efficient photovoltaic device operation. These block copolymers self-assemble to form in-plane lamellar morphologies with alternating electron donor and acceptor domains and a dominant face-on orientation in the crystalline P3HT block. Even without the

Received: April 20, 2013
Revised: May 14, 2013
Published: May 20, 2013

   dx.doi.org/10.1021/nl401420s | *Nano Lett.* 2013, 13, 2957−2963

use of fullerene, we obtain efficiencies near 3%, remarkable open-circuit voltages of 1.2 V, and short-circuit currents above 5 mA/cm^2 from block copolymer devices. These results demonstrate that conjugated block copolymers are a viable strategy for morphology and interfacial control for high performance organic solar cells.

The structure of P3HT, PFTBT, and P3HT-*b*-PFTBT are shown in Figure 1a. P3HT-*b*-PFTBT is roughly symmetric in composition with 56 wt % P3HT and a total weight-averaged molecular weight of 29 kg/mol. The energy levels of PFTBT as an electron acceptor are well aligned with those of P3HT as an electron donor, such that the difference between the lowest unoccupied molecular orbital of PFTBT (~ 3.5 eV)[24] and the highest occupied molecular orbital of P3HT (~ 4.9 eV)[25] can yield open-circuit voltages above 1 V. High open-circuit voltages have indeed been demonstrated for solar cells where the active layer is comprised of blends of P3HT and other dioctylfluorene bisthienyl-benzothiadiazole alternating copolymers,[25] ternary blends composed of similar conjugated block copolymers as P3HT-*b*-PFTBT with donor and acceptor homopolymers,[26] or polymer blends with fluorene benzothiadiazole alternating copolymers as acceptor molecules.[27−29]

Solar cell devices with P3HT/PFTBT blends as active layers are compared with devices comprised of P3HT-*b*-PFTBT block copolymers in Figure 1b. All devices have an active layer thickness of 60−70 nm and were thermally annealed after deposition of the cathode (Al). As shown in Table 1, devices made from P3HT/PFTBT blends exhibit a maximum power conversion efficiency of 1.0%, which is comparable to the performance reported previously for devices that utilize blends of P3HT and PFTBT-based polymers as the active layer.[25] Solar cells made from P3HT/PFTBT blends are optimized at 1:2 weight ratios of P3HT/PFTBT after annealing at 100 °C for 20 min. Longer annealing times or higher annealing temperatures lead to a drop in performance, potentially due to macroscopic phase separation.

If the active layer is comprised of P3HT-*b*-PFTBT block copolymers, devices yield average efficiencies of 1.5% under annealing conditions optimal for polymer blend devices (100 °C for 20 min) and higher efficiencies of around 1.7% with an extended annealing time of 90 min at 100 °C (Table 1). Optimal performance, however, is achieved at higher annealing temperatures. After annealing for 10 min at 165 °C, average power conversion efficiencies of 2.7 ± 0.4% with short-circuit currents (J_{sc}) of 5.0 ± 0.3 mA/cm^2, open-circuit voltages (V_{oc}) of 1.14 ± 0.08 V and fill factors of 0.45 ± 0.02 were measured for devices under simulated solar conditions made from block copolymers. The nearly 3-fold increase in device performance with respect to optimized devices comprised of polymer blends is due to enhancements of the short-circuit currents and fill factors. Nevertheless, fill factors in all of our devices do not exceed 0.5, a result of the inflection point near open-circuit conditions visible in the current−voltage characteristics shown in Figure 1. We attribute the presence of an inflection point to problems in charge extraction due to either an imbalance in charge transport or accumulation of charge at an interface.[30,31] As shown in Table 2, the best overall efficiency among our devices was recorded at 3.1% with an open-circuit voltage of 1.23 V. This device performance is remarkable for solar cells based on donor−acceptor block copolymers[15−17,32,33] and for nonfullerene solution-processed organic solar cells.[34−37]

The absorption spectrum of pristine P3HT-*b*-PFTBT films and external quantum efficiency (EQE) of P3HT-*b*-PFTBT devices annealed at 165 °C are shown in Figure 1c. The absorption profiles of P3HT-*b*-PFTBT films preserve the features of the constituent homopolymers and a similar optical bandgap (~2 eV) as P3HT is deduced from the absorption edge (see Figure S1 in the Supporting Information). Optimized

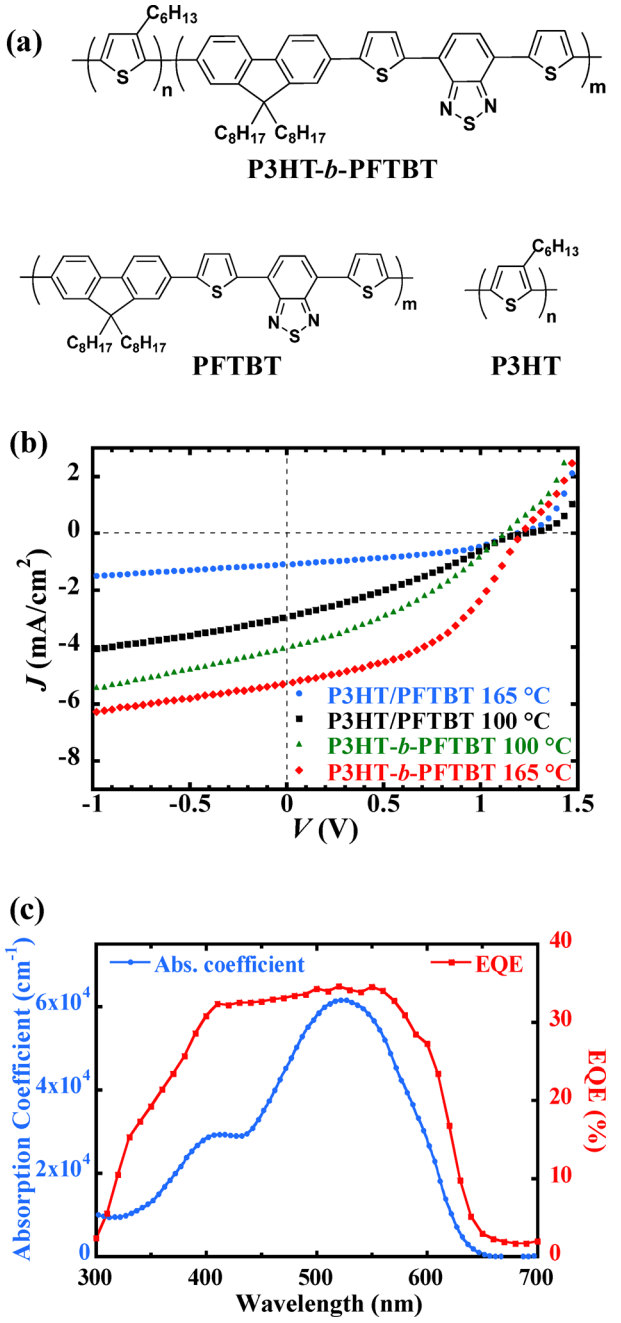

Figure 1. Photovoltaic device performances of block copolymer P3HT-*b*-PFTBT and polymer blend P3HT/PFTBT solar cells at different annealing temperatures. (a) Chemical structures of P3HT-*b*-PFTBT, PFTBT, and P3HT. (b) Current−voltage characteristics of P3HT/PFTBT (1:2 by mass) and P3HT-*b*-PFTBT photovoltaic devices annealed at 100 °C for 20 min and 165 °C for 10 min, respectively. P3HT/PFTBT solar cells are optimized at 100 °C for 20 min, while P3HT-*b*-PFTBT devices are optimized at 165 °C for 10 min. Devices were measured under simulated AM 1.5G irradiation with intensity of 97 mW/cm^2. (c) UV−visible absorption spectrum of a P3HT-*b*-PFTBT film and EQE characteristics of a P3HT-*b*-PFTBT solar cell annealed at optimized conditions (165 °C for 10 min).

dx.doi.org/10.1021/nl401420s | *Nano Lett.* 2013, 13, 2957−2963

Table 1. Device Characteristics[a] of P3HT/PFTBT Blend and P3HT-*b*-PFTBT Block Copolymer Solar Cells at Different Annealing Conditions

	efficiency (%)	short-circuit current (mA/cm^2)	open-circuit voltage (V)	fill factor
100 °C 20 min polymer blend	1.0 ± 0.1	2.6 ± 0.3	1.22 ± 0.02	0.33 ± 0.02
165 °C 10 min polymer blend	0.5 ± 0.1	1.0 ± 0.1	1.16 ± 0.03	0.42 ± 0.02
100 °C 20 min block copolymer	1.5 ± 0.1	3.7 ± 0.2	1.13 ± 0.04	0.35 ± 0.01
100 °C 90 min block copolymer	1.7 ± 0.1	4.1 ± 0.1	1.14 ± 0.02	0.35 ± 0.01
165 °C 10 min block copolymer	2.7 ± 0.4	5.0 ± 0.3	1.14 ± 0.08	0.45 ± 0.02

[a]Under simulated AM 1.5G irradiation with intensity of 97 mW/cm^2.

Table 2. Device Characteristics[a] of P3HT/PFTBT Polymer Blend and P3HT-*b*-PFTBT Block Copolymer Solar Cells with Highest Efficiencies

	efficiency (%)	short-circuit current (mA/cm^2)	open-circuit voltage (V)	fill factor
best device, block copolymer	3.1	5.2	1.23	0.47
best device, blend	1.1	2.9	1.22	0.30

[a]Under simulated AM 1.5G irradiation with intensity of 97 mW/cm^2.

block copolymer devices display relatively high photoconversion efficiencies over a broad range of wavelengths (namely 350−610 nm) with EQE values of 20−35%, which are significant for thin-film photovoltaics based on only polymeric materials. Interestingly, an EQE value of 31% was recorded at 400 nm where the exciton generation is mostly attributed to the optical absorption of PFTBT, suggesting efficient exciton dissociation from photoexcitations in the acceptor domains. Integrating the EQE results predicts a J_{sc} of 4.7 mA/cm^2 with an AM 1.5G reference spectrum. This is consistent with a measured J_{sc} of 5.0 mA/cm^2 under AM 1.5G simulated solar conditions for the same device (~5% error). We attribute the small discrepancy to degradation in air, as EQE measurements took place in ambient. Indeed, devices that have undergone EQE measurements exhibit reduced J_{sc}'s (<4 mA/cm^2) when tested under 1 sun conditions in a N_2 atmosphere.

Resonant soft X-ray scattering (RSOXS) and grazing-incidence X-ray scattering measurements were carried out to elucidate the basis for the enhanced performance of block copolymer devices compared to devices made from polymer blends. RSOXS is a powerful tool for characterizing the phase separation in polymer thin films with limited phase contrast or in complicated multiphase systems.[38−41] Differences in the core electronic transitions of organic materials in the soft X-ray regime greatly enhance scattered intensities over hard X-ray scattering, enabling transmission X-ray scattering experiments of thin polymer films. As shown in Figure S2 of the Supporting Information, the X-ray absorptions of P3HT and PFTBT differ at 285.4 eV, which enables RSOXS experiments.

Figure 2 presents RSOXS intensities as a function of scattering vector, q ($q = 4\pi \sin(\theta/2)/\lambda$, λ is the X-ray wavelength and θ is the scattering angle), taken at 285.4 eV X-ray energy for P3HT/PFTBT polymer blend and P3HT-*b*-PFTBT block copolymer thin films annealed at 100 and 165 °C, respectively. The film annealing conditions match the optimum for the active layer of devices. Scattering data from polymer blends show little structure. Scattering profiles from P3HT-*b*-PFTBT block copolymer films are distinct from scattering data from polymer blends (Figure 2 and Figure S3 of the Supporting Information) or polymer/fullerene mixtures.[10,42] A primary scattering peak at $q^* = 0.035$ Å^{-1} and a weak second-order peak at $2q^* = 0.070$ Å^{-1} are evident in data from thin films of block copolymers annealed at 165 °C. The positions of the scattering peaks at q^* and $2q^*$ are a signature of self-assembly into block copolymer lamellar microdomains[43,44] with a domain spacing of approximately 18 nm. The individual domain sizes are therefore roughly 9 nm, comparable to the exciton diffusion length in organic semiconductors (~10 nm).[45]

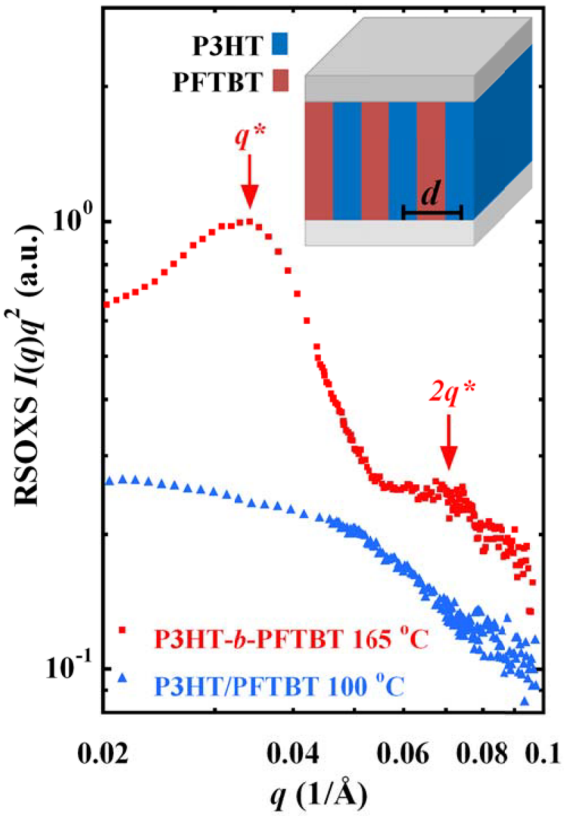

Figure 2. Comparison of the morphology in the active layers of optimized P3HT-*b*-PFTBT and P3HT/PFTBT photovoltaic devices using RSOXS. RSOXS data were acquired at the carbon absorption edge (285.4 eV) of a P3HT-*b*-PFTBT film annealed at 165 °C and a P3HT/PFTBT (1:2 by mass) blend annealed at 100 °C. RSOXS intensities are offset for clarity. Scattering data are presented as a Kratky plot of $I(q)q^2$ vs q, where $I(q)$ is the scattering intensity and q is the scattering vector. In optimized P3HT-*b*-PFTBT samples, a well-defined primary peak, q^* (~0.035 Å^{-1}), and second-order reflection, $2q^*$, are identified. Schematic illustration of the lamellar morphology is shown in the inset with the average domain spacing indicated as d.

RSOXS experiments in the transmission geometry exclusively explore the in-plane film structure and consequently demonstrate the presence of P3HT-*b*-PFTBT lamellae oriented perpendicular to the substrate, as shown in the inset of Figure 2. Grazing incidence small-angle X-ray scattering (GISAXS) measurements shown in Figure S4 of the Supporting Information similarly suggest in-plane microdomains with

dx.doi.org/10.1021/nl401420s | Nano Lett. 2013, 13, 2957−2963

roughly 16 nm spacing (q^* = 0.04 Å^{-1}), in reasonable agreement with the length scales extracted from RSOXS data. Consequently, RSOXS and GISAXS data demonstrate a thin-film lamellar morphology that not only establishes an equilibrium microstructure amenable for exciton dissociation but also provides pathways for electron and hole transport to the corresponding electrodes. We note that the appearance of a lamellar microstructure in P3HT-*b*-PFTBT films only occurs at 165 °C and not 100 °C (see Figure S3 of the Supporting Information), and device efficiencies exhibit a roughly 2-fold increase when films are annealed at 165 °C versus 100 °C (Table 1). Thus, we attribute the significant improvement in photovoltaic device performance to the self-assembly of block copolymers into well-defined mesostructures in the active layer.

We examined the molecular order in block copolymer thin films using conventional X-ray diffraction (XRD) and grazing-incidence wide-angle X-ray scattering (GIWAXS). Measurements were performed on P3HT-*b*-PFTBT films deposited on top of PEDOT:PSS-coated Si substrates and processed in an analogous manner to optimized devices (165 °C annealing for 10 min). XRD results show that PFTBT is amorphous while P3HT forms crystalline structures in both blend and block copolymer films with the same (100) spacing as that in pristine P3HT films (Figure 3a). Complementary 2D GIWAXS measurements provide the preferred orientation of these crystallites through analysis of both the in-plane (along q_y) and out-of-plane (along q_z) scattering data. As shown in Figure 3b, the (100), (200), and (300) reflections of P3HT ($q \sim 0.4$, 0.8, and 1.2 Å^{-1}, respectively), corresponding to spacing between the polymer backbone through the alkyl side-chains, are strongly in-plane with the substrate (along q_y). The (010) peak ($q \sim 1.65$ Å^{-1}), which corresponds to π–π stacking between chains, is only evident in the out-of-plane direction (along q_z). This indicates that P3HT assumes a predominantly face-on orientation with π-stacking primarily out-of-plane with the substrate. Face-on P3HT crystallites likely enhance the hole extraction efficacy because the fast charge transport direction is along the π–π stacking direction.[46] The orientation of P3HT crystals in P3HT-*b*-PFTBT block copolymer films differs qualitatively from previously reported studies on P3HT crystallization in homopolymers,[47] polymer/fullerene mixtures,[48,49] or polymer/polymer blends[50] where edge-on orientations are strongly preferred. To first order, there is no reason for the lamellar block copolymer morphology to constrain the P3HT block into either a face-on or edge-on orientation. Instead, we hypothesize that interactions between PFTBT and the substrate lead to preferred face-on orientations for the PFTBT block at the substrate interface. Consequently, the connectivity between blocks nucleates crystals with face-on orientations within the P3HT domains.

The combination of our device results and structural characterization on multiple length scales demonstrates the unique strengths of block copolymer architectures for efficient organic photovoltaics. In addition to controlling the mesoscale structure, conjugated block copolymers provide control of the donor–acceptor interface and of crystallite orientations. Covalent bonding across the donor–acceptor interface has the potential to control charge separation and charge recombination rates,[51,52] opening the possibility of achieving the near unit efficiencies for charge separation from charge transfer states observed in photosynthetic systems.[53] In our studies, the device performance increases when the active layer is composed of block copolymers instead of polymer blends

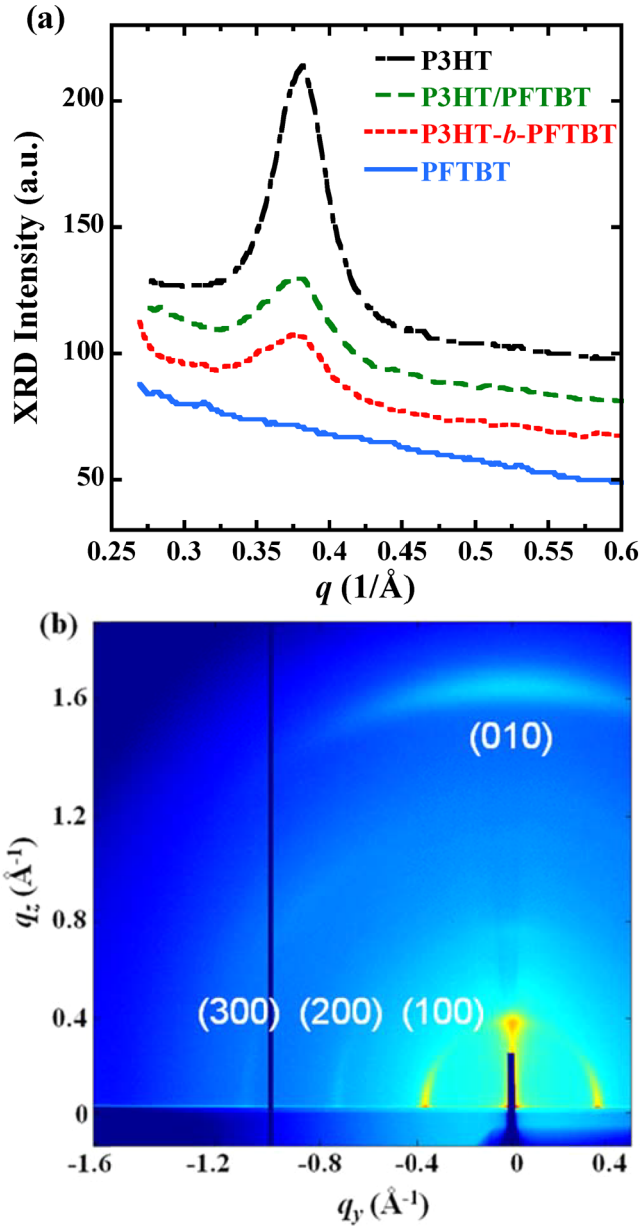

Figure 3. Molecular organization in P3HT-*b*-PFTBT thin films. (a) X-ray diffraction (XRD) patterns of neat P3HT, neat PFTBT, P3HT/PFTBT blend, and P3HT-*b*-PFTBT block copolymer films annealed at 165 °C. (b) Two-dimensional GIWAXS pattern for thin films of P3HT-*b*-PFTBT annealed at optimized conditions (165 °C) for device performance. The (100), (200), and (300) diffraction peaks of regioregular P3HT are strongly biased in the in-plane direction (q_y) and the (010) peak is apparent in the out-of-plane direction (q_z), suggesting face-on crystallites.

even when the morphology is roughly invariant between the two systems; for example, after annealing at 100 °C the device efficiencies improve by 50% when block copolymers are used as active layers even though the RSOXS data and mesoscale structures are similar for block copolymer and blend films (Table 1 and Figure S3 of the Supporting Information). A possible explanation for the difference in the device performance between blend and block copolymer devices is that the connectivity between blocks provides donor/acceptor interfaces within length scales of the order of chain dimensions (ca. 10 nm) and consequently promotes charge separation. The size

dx.doi.org/10.1021/nl401420s | *Nano Lett.* 2013, 13, 2957–2963

of domains, however, in P3HT/PFTBT blends at optimum conditions is near 10−20 nm, as evident from the inflection point in the scattering data from blends shown in Figure 2 or RSOXS data in ref 54. Another possible explanation, changes in charge extraction efficacy, is ruled out given that the current at reverse bias scales with the short-circuit current in Figure 1b.[42] Thus, we hypothesize that conjugation across the donor−acceptor interface is responsible for enhancing device performance in block copolymer devices even when the microstructure of the active layer is similar to blends, suggesting that covalent control of donor−acceptor interfaces is a route for controlling interfacial molecular order, exciton dissociation and charge recombination to enhance excitonic solar cell performance.

Establishing exceptional performance in P3HT-*b*-PFTBT solar cells provides a clear pathway for enhancing efficiencies in fully conjugated block copolymers devices. The choice of P3HT and PFTBT as constituent blocks is motivated by previous work on optimizing polymer blends composed of P3HT and PFTBT derivatives for the active layer of solar cells.[25,55−58] As a consequence, combinations of polymer blocks with complementary absorbance could lead to significant enhancements in short-circuit currents beyond P3HT-*b*-PFTBT because the absorption spectra of P3HT and PFTBT overlap significantly (Figure S1 of the Supporting Information). Broad-band light absorption can be achieved in combination with open-circuit voltages beyond 1 V with careful design of the HOMO/LUMO levels of the constituent blocks, as demonstrated with P3HT-*b*-PFTBT. Previous work has also demonstrated the presence of exciplex or bound charge transfer states at polymer−polymer interfaces that are unlikely to contribute to the photocurrent at room temperature.[59−61] These strongly bound states are localized, in many cases intermolecularly to the benzothiadiazole group in the acceptor polymer.[62,63] Nevertheless, recent photophysical studies of conjugated donor−acceptor molecules have shown that the presence of localized charge transfer states and consequently the degree of recombination depend strongly on the linking chemistry.[64] As such, fully conjugated block copolymers provide a path to achieve unprecedented combinations of light absorption, high photovoltages, and control of electronic coupling at donor−acceptor interfaces in single-component active layers of organic solar cells.

Materials and Methods. Regioregular P3HT (96% H-T regioregular, M_n = 26 kg/mol, polydispersity = 2.0) was purchased from Merck. All other reagents and solvents were purchased from Sigma-Aldrich and used as received. P3HT-*b*-PFTBT block copolymers were synthesized using a procedure similar to that previously described[23] and the synthesis is briefly discussed in the Supporting Information (Section 4, Synthesis of Block Copolymers).

Photovoltaic devices were prepared with the conventional architecture of ITO/PEDOT/:PSS (65 nm)/active layer (60−70 nm)/Al (75 nm). ITO-coated glass substrates (20 ohm/sq, Xin Yan Technology, Hong Kong) were cleaned by soap, followed by 20 min of sonication in acetone, then isopropanol, and finally 15 min of ultraviolet light ozonation. Poly(3,4-ethylenedioxythiophene) poly(styrenesulfonate), PEDOT:PSS (Clevios P, Heraeus), was spin-coated on top of ITO at 4000 rpm for 2 min yielding a thickness of about 65 nm. The PEDOT:PSS/ITO substrates were dried for 10 min at 165 °C in air and then transferred to a nitrogen-filled glovebox. Solutions of P3HT/PFTBT mixtures (15 mg/mL, weight ratio 1:2) and P3HT-*b*-PFTBT (5 mg/mL) were made with anhydrous chloroform (≥ 99%, amylenes as stabilizer, Sigma-Aldrich) and stirred at 95 °C for about 20−22 h in a tightly sealed container prior to casting in a N_2 glovebox. The active layers of P3HT/PFTBT and P3HT-*b*-PFTBT devices were cast onto PEDOT:PSS layers from prepared hot solutions (95 °C) at various spin speeds for 1 min to maintain thicknesses around 60−70 nm. The film thicknesses were determined on a TENCOR P-10 surface profiler. Samples were then transferred immediately onto a calibrated digital hot plate at 100 or 165 °C and dried for 5 min. The devices were completed by vacuum thermal evaporation of 75 nm aluminum at 10^{-6} Torr on top of the active layer through a shadow mask. The device area is 16.2 mm^2. Integrated solar cells were further annealed at 100 or 165 °C for various annealing times.

Photovoltaic measurements were performed in a N_2 atmosphere under simulated AM 1.5G illumination (97 mW/cm^2) from a xenon lamp solar simulator (Newport Model SP92250A-1000). The illumination intensity was calibrated using an optical power meter and NREL certified Si reference photocell (Newport). A Keithley 2636A Sourcemeter was used to measure the current−voltage characteristics of solar cells. External quantum efficiencies (EQE) were measured in air. The photocurrents as a function of wavelength were recorded by a multifunction optical power meter (Model 70310) using 300 W xenon lamp and Cornerstone monochromator (Newport Model 74100) illumination. The absorption spectra of films were measured using an ultraviolet/visible/near-infrared spectrophotometer (Beckman DU Series 500).

Samples for RSOXS, XRD, GISAXS, and GIWAXS measurements were prepared on PEDOT:PSS/Si substrates in the same manner as for device fabrication. For RSOXS experiments, as-cast films were floated-off in deionized water and picked up with 5 mm × 5 mm silicon frames supporting a 1 mm × 1 mm, 100 nm thick Si_3N_4 window. Samples were then dried for 24 h at room temperature under vacuum and subsequently annealed on a hot plate in the N_2 glovebox. RSOXS measurements were carried out at beamline 11.0.1.2 at the Advanced Light Source, Lawrence Berkeley National Laboratory.[65] Scattering was performed in the transmission geometry in vacuum at the carbon absorption edge X-ray energies (285.4 eV) with linearly polarized X-rays. Data were corrected for dark currents and azimuthally integrated.

XRD experiments were conducted at the Materials Characterization Lab of the Pennsylvania State University on a Rigaku DMAX Rapid Microdiffractometer. The X-ray wavelength, λ, was 1.54 Å. Rocking curves were obtained by rocking the sample (±0.5°) around the Bragg angle and images were collected with a curved image plate detector. Data were azimuthally integrated. GISAXS and GIWAXS measurements were carried out at Beamline 8-ID-E of the Advanced Photon Source, Argonne National Laboratory (λ = 1.6868 Å).[66] Scattering data were acquired at an incident angle of 0.2°. Data were corrected for X-ray polarization, detector sensitivity, and geometrical solid-angle.

■ ASSOCIATED CONTENT

Supporting Information

Details on device characteristics, optical and X-ray absorption spectra, GISAXS and RSOXS data, synthetic details of block copolymers, and size-exclusion chromatography traces. This material is available free of charge via the Internet at http://pubs.acs.org.

AUTHOR INFORMATION

Corresponding Author

*E-mail: (E.D.G.) edg12@psu.edu; (R.V) rafaelv@rice.edu.

Author Contributions

[¶]C.G. and Y.H.L. contributed equally to this work.

Notes

The authors declare no competing financial interests.

ACKNOWLEDGMENTS

C.G., M.D.W., and E.D.G. acknowledge financial support from NSF under Award DMR-1056199. The Advanced Light Source is supported by the Director, Office of Science, Office of Basic energy Sciences, of the U.S. Department of Energy under Contract No. DE-AC02-05CH11231. Use of the Advanced Photon Source is supported by the U.S. Department of Energy, Office of Science, Office of Basic Energy Sciences, under Contract No. DE-AC02-06CH11357. R.V., K.A.S., and Y.H.L. acknowledge support from the Welch Foundation for Chemical Research (Grant C-1750), the Shell Center for Sustainability, and Louis and Peaches Owen. The authors acknowledge John Asbury at the Pennsylvania State University for use of his UV−vis spectrometer.

REFERENCES

(1) Brédas, J.-L.; Norton, J. E.; Cornil, J.; Coropceanu, V. *Acc. Chem. Res.* **2009**, *42* (11), 1691−1699.

(2) Forrest, S. R. *Nature* **2004**, *428* (6986), 911−918.

(3) Shaheen, S. E.; Ginley, D. S.; Jabbour, G. E. *MRS Bull.* **2005**, *30* (1), 10−19.

(4) Mayer, A. C.; Scully, S. R.; Hardin, B. E.; Rowell, M. W.; McGehee, M. D. *Mater. Today* **2007**, *10* (11), 28−33.

(5) Giebink, N. C.; Wiederrecht, G. P.; Wasielewski, M. R.; Forrest, S. R. *Phys. Rev. B* **2010**, *82* (15), 155305.

(6) Thompson, B. C.; Fréchet, J. M. J. *Angew. Chem., Int. Ed.* **2008**, *47* (1), 58−77.

(7) Chen, W.; Nikiforov, M. P.; Darling, S. B. *Energy Environ. Sci.* **2012**, *5* (8), 8045−8074.

(8) Kim, J. B.; Allen, K.; Oh, S. J.; Lee, S.; Toney, M. F.; Kim, Y. S.; Kagan, C. R.; Nuckolls, C.; Loo, Y. L. *Chem. Mater.* **2010**, *22* (20), 5762−5773.

(9) Vakhshouri, K.; Kozub, D. R.; Wang, C.; Salleo, A.; Gomez, E. D. *Phys. Rev. Lett.* **2012**, *108* (2), 026601.

(10) Kozub, D. R.; Vakhshouri, K.; Orme, L. M.; Wang, C.; Hexemer, A.; Gomez, E. D. *Macromolecules* **2011**, *44* (14), 5722−5726.

(11) Brabec, C. J.; Gowrisanker, S.; Halls, J. J. M.; Laird, D.; Jia, S.; Williams, S. P. *Adv. Mater.* **2010**, *22* (34), 3839−3856.

(12) Xin, H.; Reid, O. G.; Ren, G. Q.; Kim, F. S.; Ginger, D. S.; Jenekhe, S. A. *ACS Nano* **2010**, *4* (4), 1861−1872.

(13) Bates, F. S.; Fredrickson, G. H. *Phys. Today* **1999**, *52* (2), 32−38.

(14) Leibler, L. *Macromolecules* **1980**, *13* (6), 1602−1617.

(15) Sary, N.; Richard, F.; Brochon, C.; Leclerc, N.; Leveque, P.; Audinot, J. N.; Berson, S.; Heiser, T.; Hadziioannou, G.; Mezzenga, R. *Adv. Mater.* **2010**, *22* (6), 763−768.

(16) Zhang, Q. L.; Cirpan, A.; Russell, T. P.; Emrick, T. *Macromolecules* **2009**, *42* (4), 1079−1082.

(17) Tao, Y. F.; McCulloch, B.; Kim, S.; Segalman, R. A. *Soft Matter* **2009**, *5* (21), 4219−4230.

(18) Sivula, K.; Ball, Z. T.; Watanabe, N.; Frechet, J. M. J. *Adv. Mater.* **2006**, *18* (2), 206−210.

(19) Sun, S. S.; Zhang, C.; Ledbetter, A.; Choi, S.; Seo, K.; Bonner, C. E.; Drees, M.; Sariciftci, N. S. *Appl. Phys. Lett.* **2007**, *90*, 043117.

(20) Hadziioannou, G. *MRS Bull.* **2002**, *27*, 456−460.

(21) Ku, S.-Y.; Brady, M. A.; Treat, N. D.; Cochran, J. E.; Robb, M. J.; Kramer, E. J.; Chabinyc, M. L.; Hawker, C. J. *J. Am. Chem. Soc.* **2012**, *134* (38), 16040−16046.

(22) Sommer, M.; Komber, H.; Huettner, S.; Mulherin, R.; Kohn, P.; Greenham, N. C.; Huck, W. T. S. *Macromolecules* **2012**, *45* (10), 4142−4151.

(23) Lin, Y.-H.; Smith, K. A.; Kempf, C. N.; Verduzco, R. *Polym. Chem.* **2013**, *4* (2), 229−232.

(24) Zhang, F. L.; Perzon, E.; Wang, X. J.; Mammo, W.; Andersson, M. R.; Inganas, O. *Adv. Funct. Mater.* **2005**, *15* (5), 745−750.

(25) McNeill, C. R.; Halls, J. J. M.; Wilson, R.; Whiting, G. L.; Berkebile, S.; Ramsey, M. G.; Friend, R. H.; Greenham, N. C. *Adv. Funct. Mater.* **2008**, *18* (16), 2309−2321.

(26) Mulherin, R. C.; Jung, S.; Huettner, S.; Johnson, K.; Kohn, P.; Sommer, M.; Allard, S.; Scherf, U.; Greenham, N. C. *Nano Lett.* **2011**, *11* (11), 4846−4851.

(27) Ramsdale, C. M.; Barker, J. A.; Arias, A. C.; MacKenzie, J. D.; Friend, R. H.; Greenham, N. C. *J. Appl. Phys.* **2002**, *92* (8), 4266−4270.

(28) Barker, J. A.; Ramsdale, C. M.; Greenham, N. C. *Phys. Rev. B* **2003**, *67* (7), 075205.

(29) Snaith, H. J.; Greenham, N. C.; Friend, R. H. *Adv. Mater.* **2004**, *16* (18), 1640−1645.

(30) Tress, W.; Petrich, A.; Hummert, M.; Hein, M.; Leo, K.; Riede, M. *Appl. Phys. Lett.* **2011**, *98* (6), 063301.

(31) Wang, J. C.; Ren, X. C.; Shi, S. Q.; Leung, C. W.; Chan, P. K. L. *Org. Electron.* **2011**, *12* (6), 880−885.

(32) Miyanishi, S.; Zhang, Y.; Tajima, K.; Hashimoto, K. *Chem. Commun.* **2010**, *46* (36), 6723−6725.

(33) Topham, P. D.; Parnell, A. J.; Hiorns, R. C. *J. Polym. Sci., Part B: Polym. Phys.* **2011**, *49* (16), 1131−1156.

(34) Anthony, J. E. *Chem. Mater.* **2011**, *23* (3), 583−590.

(35) Sonar, P.; Lim, J. P. F.; Chan, K. L. *Energy Environ. Sci.* **2011**, *4* (5), 1558−1574.

(36) Mikroyannidis, J. A.; Suresh, P.; Sharma, G. D. *Synth. Met.* **2010**, *160* (9−10), 932−938.

(37) Ahmed, E.; Ren, G. Q.; Kim, F. S.; Hollenbeck, E. C.; Jenekhe, S. A. *Chem. Mater.* **2011**, *23* (20), 4563−4577.

(38) Virgili, J. M.; Tao, Y.; Kortright, J. B.; Balsara, N. P.; Segalman, R. A. *Macromolecules* **2007**, *40* (6), 2092−2099.

(39) Wang, C.; Lee, D. H.; Hexemer, A.; Kim, M. I.; Zhao, W.; Hasegawa, H.; Ade, H.; Russell, T. P. *Nano Lett.* **2011**, *11* (9), 3906−3911.

(40) Swaraj, S.; Wang, C.; Yan, H. P.; Watts, B.; Jan, L. N.; McNeill, C. R.; Ade, H. *Nano Lett.* **2010**, *10* (8), 2863−2869.

(41) Guo, C.; Kozub, D. R.; Vajjala Kesava, S.; Wang, C.; Hexemer, A.; Gomez, E. D. *ACS Macro Lett.* **2013**, *2*, 185−189.

(42) Kozub, D. R.; Vakhshouri, K.; Kesava, S. V.; Wang, C.; Hexemer, A.; Gomez, E. D. *Chem. Commun.* **2012**, *48* (47), 5859−5861.

(43) Bendejacq, D.; Ponsinet, V.; Joanicot, M.; Loo, Y. L.; Register, R. A. *Macromolecules* **2002**, *35* (17), 6645−6649.

(44) Hamley, I. W. *The Physics of Block Copolymers*; Oxford University Press: Oxford, 1998.

(45) Haugeneder, A.; Neges, M.; Kallinger, C.; Spirkl, W.; Lemmer, U.; Feldmann, J.; Scherf, U.; Harth, E.; Gugel, A.; Mullen, K. *Phys. Rev. B* **1999**, *59* (23), 15346−15351.

(46) Sirringhaus, H.; Brown, P. J.; Friend, R. H.; Nielsen, M. M.; Bechgaard, K.; Langeveld-Voss, B. M. W.; Spiering, A. J. H.; Janssen, R. A. J.; Meijer, E. W.; Herwig, P.; de Leeuw, D. M. *Nature* **1999**, *401* (6754), 685−688.

(47) Yang, H. C.; Shin, T. J.; Yang, L.; Cho, K.; Ryu, C. Y.; Bao, Z. N. *Adv. Funct. Mater.* **2005**, *15* (4), 671−676.

(48) Woo, C. H.; Thompson, B. C.; Kim, B. J.; Toney, M. F.; Frechet, J. M. J. *J. Am. Chem. Soc.* **2008**, *130* (48), 16324−16329.

(49) Li, G.; Yao, Y.; Yang, H.; Shrotriya, V.; Yang, G.; Yang, Y. *Adv. Funct. Mater.* **2007**, *17* (10), 1636−1644.

(50) Nam, S.; Shin, M.; Park, S.; Lee, S.; Kim, H.; Kim, Y. *Phys. Chem. Chem. Phys.* **2012**, *14* (43), 15046−15053.

(51) Bu, L.; Guo, X.; Yu, B.; Qu, Y.; Xie, Z.; Yan, D.; Geng, Y.; Wang, F. *J. Am. Chem. Soc.* **2009**, *131* (37), 13242−13243.

(52) Guo, Z. Y.; Jenekhe, S. A.; Prezhdo, O. V. *Phys. Chem. Chem. Phys.* **2011**, *13* (17), 7630−7636.
(53) Blankenship, R. E. *Molecular Mechanisms of Photosynthesis*; Blackwell Science: Oxford, U.K., 2002.
(54) Yan, H. P.; Collins, B. A.; Gann, E.; Wang, C.; Ade, H.; McNeill, C. R. *ACS Nano* **2012**, *6* (1), 677−688.
(55) McNeill, C. R.; Abrusci, A.; Zaumseil, J.; Wilson, R.; McKiernan, M. J.; Burroughes, J. H.; Halls, J. J. M.; Greenham, N. C.; Friend, R. H. *Appl. Phys. Lett.* **2007**, *90* (19), 193506−3.
(56) McNeill, C. R.; Westenhoff, S.; Groves, C.; Friend, R. H.; Greenham, N. C. *J. Phys. Chem. C* **2007**, *111* (51), 19153−19160.
(57) McNeill, C. R.; Abrusci, A.; Hwang, I.; Ruderer, M. A.; Müller-Buschbaum, P.; Greenham, N. C. *Adv. Funct. Mater.* **2009**, *19* (19), 3103−3111.
(58) McNeill, C. R.; Greenham, N. C. *Adv. Mater.* **2009**, *21* (38−39), 3840−3850.
(59) Morteani, A. C.; Dhoot, A. S.; Kim, J. S.; Silva, C.; Greenham, N. C.; Murphy, C.; Moons, E.; Cina, S.; Burroughes, J. H.; Friend, R. H. *Adv. Mater.* **2003**, *15* (20), 1708−1712.
(60) Friend, R. H.; Phillips, M.; Rao, A.; Wilson, M. W. B.; Li, Z.; McNeill, C. R. *Faraday Discuss.* **2012**, *155*, 339−348.
(61) Yin, C. H.; Kietzke, T.; Kumke, M.; Neher, D.; Horhold, H. H. *Sol. Energy Mater. Sol. Cells* **2007**, *91* (5), 411−415.
(62) Huang, Y. S.; Westenhoff, S.; Avilov, I.; Sreearunothai, P.; Hodgkiss, J. M.; Deleener, C.; Friend, R. H.; Beljonne, D. *Nat. Mater.* **2008**, *7* (6), 483−489.
(63) Bakulin, A. A.; Rao, A.; Pavelyev, V. G.; van Loosdrecht, P. H. M.; Pshenichnikov, M. S.; Niedzialek, D.; Cornil, J.; Beljonne, D.; Friend, R. H. *Science* **2012**, *335* (6074), 1340−1344.
(64) Johnson, K.; Huang, Y.-S.; Huettner, S.; Sommer, M.; Brinkmann, M.; Mulherin, R.; Niedzialek, D.; Beljonne, D.; Clark, J.; Huck, W. T. S.; Friend, R. H. *J. Am. Chem. Soc.* **2013**, *135* (13), 5074−5083.
(65) Gann, E.; Young, A. T.; Collins, B. A.; Yan, H.; Nasiatka, J.; Padmore, H. A.; Ade, H.; Hexemer, A.; Wang, C. *Rev. Sci. Instrum.* **2012**, *83* (4), 045110.
(66) Jiang, Z.; Li, X.; Strzalka, J.; Sprung, M.; Sun, T.; Sandy, A. R.; Narayanan, S.; Lee, D. R.; Wang, J. *J. Synchrotron Radiat.* **2012**, *19*, 627−636.